Pis'ma v ZhETF, vol. 99, iss. 1, pp. 19 – 24

On nonlinear cascades and resonances in the outer magnetosphere

S. Savin[a1)], *E. Amata*[b], *V. Budaev*[a,g], *L. Zelenyi*[a], *E. A. Kronberg*[c], *J. Buechner*[c], *J. Safrankova*[d], *Z. Nemecek*[d], *J. Blecki*[e], *L. Kozak*[f], *S. Klimov*[a], *A. Skalsky*[a], *L. Lezhen*[a]

[a] *IKI, Lab545, Moscow, Russia*

[b] *IFSI, Roma, Italy*

[c] *Max-Planck Institute for Solar System Research, 70569 Stuttgart, Germany*

[d] *Charles University, 11636 Prague, Czech Republic*

[e] *Space Research Center, 57622 Warsaw, Poland*

[f] *Kyiv Taras Shevchenko University, 01601 Kyiv, Ukraine*

[g] *National Research Centre Kurchatov Institute, 123182 Moscow, Russia*

Submitted 17 July 2013
Resubmitted 21 Desember 2013

The paper addresses nonlinear phenomena that control the interaction between plasma flow (solar wind) and magnetic barrier (magnetosphere). For the first time we demonstrate that the dominant solar wind kinetic energy: (1) excites boundary resonances and their harmonics which modulate plasma jets under the bow shock; (2) produces discrete 3-wave cascades, which could merge into a turbulent-like one; (3) jet produced cascades provide the effective anomalous plasma transport inside and out of the magnetosphere; (4) intermittency and multifractality characteristics for the statistic properties of jets result in a super-ballistic turbulent transport regime. Our results could be considered as suggestive for the space weather predictions, for turbulent cascades in different media and for the laboratory plasma confinement (e.g. for fusion devices).

DOI: 10.7868/S0370274X14010044

Introduction. Interaction of the variable solar wind (SW) plasma flow with the Earth's magnetopause (MP – magnetospheric boundary) includes bow shock (BS) and turbulent magnetosheath (MSH) behind it (see the Inset in Fig. 1) [1]. The excited turbulence is often non-equilibrium, intermittent and non-stationary including plasma jets with the dynamic pressure being higher than that of SW. BS, MP and MSH possess numerous eigen modes: from membrane and cavity modes (0.2–10 mHz, described below) till ion cyclotron fluctuations (0.05–0.5 Hz). So, for a comprehensive understanding of turbulence properties one needs to fulfill multi-point multi-scale study with the simultaneous SW monitoring. We present such a case when the disturbed SW plasma flow drives directly MSH fluctuations and also pumps energy into resonant oscillations of the boundaries. Here we explore the spectral and statistical properties of the energy flow by analyzing the time series and wavelet spectra of the dominating dynamic pressure (P_{dyn}) taken at four different locations on spacecraft (s/c) DOUBLE STAR (DS), CLUSTER-4 (C4), GEOTAIL (GE), and ACE.

Multi-spacecraft data. In previous papers (see, e.g., [2–6] and references therein) the energy and plasma transfer has been studied without distinction between discrete from turbulent cascades. Usually observations of magnetic fluctuations were used to analyze the properties of plasma waves in space. Note that in the case considered here, the energy of magnetic fluctuations is, however, small versus that of the dynamic pressure studied here. In Inset of Fig. 1 one can see the s/c configuration: DS is in the subsolar MSH/ BS/ MP region, C4 comes from foreshock towards MP, GE proceeds from MP towards MSH, ACE monitors the SW in L1 Lagrangian point in front of the Earth. Foreshock is located in front of BS being alongated the SW magnetic field. Fig. 1 shows the dynamic pressure, P_{dyn}, from 3 s/c (1, 3 and 4 bottom panels), C4 energetic O^+ (originating from ionosphere, 2_{nd} bottom panel) and the ratio of the sunward magnetic field to its module ($|B_x|/|\mathbf{B}|$, top panel) on C4. Here we define the most intensive plasma jets – Super-magnetosonic Plasma Streams (SPS) – as spikes in P_{dyn} with an amplitude exceeding three stan-

1)e-mail: ssavin@iki.rssi.ru

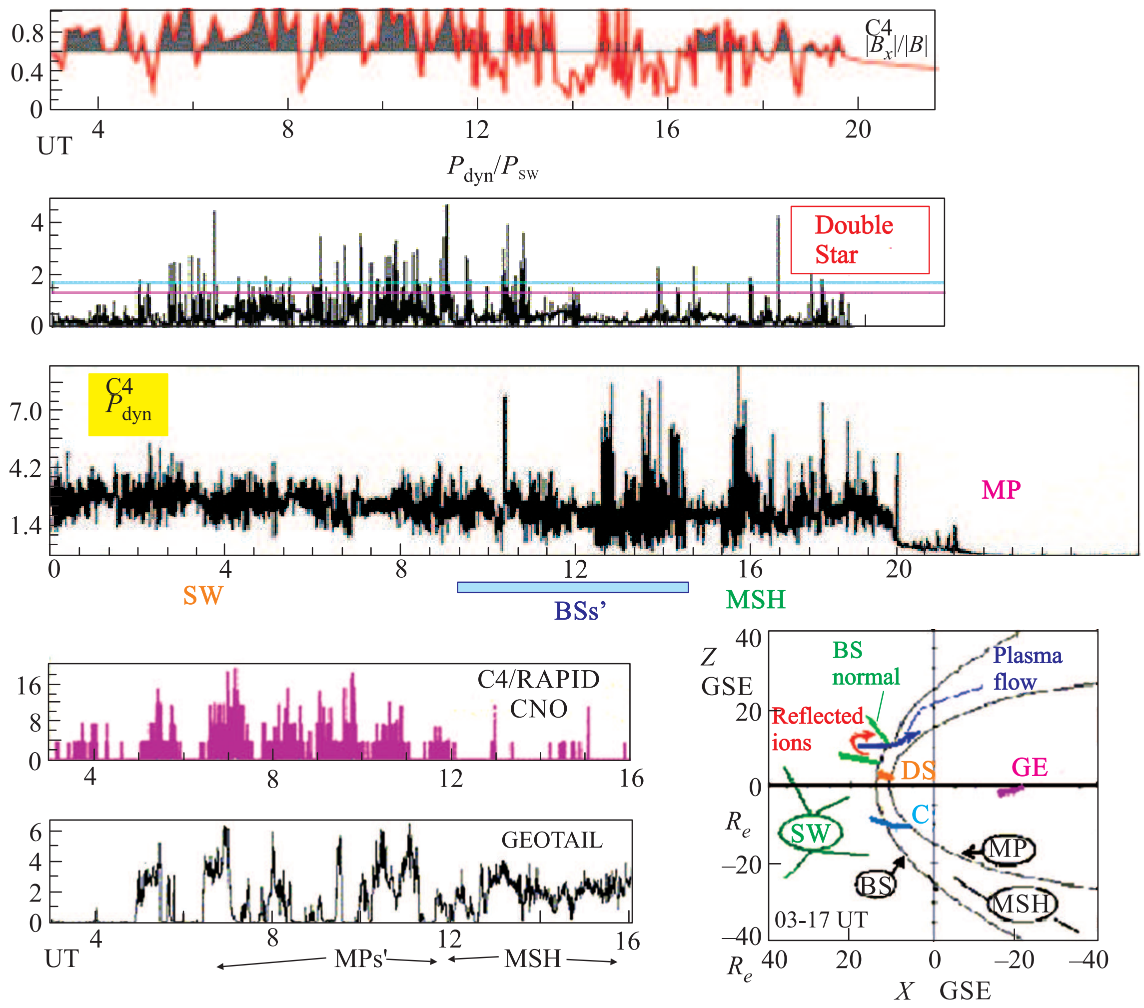

Fig. 1. March 27, 2005, from top to bottom: CLUSTER-4 (C4) s/c, magnetic field $|B_x|/|\mathbf{B}|$ with the X axis pointing at the Sun (see Inset). The shadowing indicates times during which $|B_x|/|\mathbf{B}| > 0.5$; Dynamic pressure normalized by the SW pressure, $P_{\rm dyn}/P_{\rm SW}$; obtained by observations of the DOUBLE STAR (DS) s/c at a sampling rate of 4 s; C4 s/c, $P_{\rm dyn}$; C4 s/c, CNO – channel of energetic particles (>274 keV, C^+, N^+ and O^+, units – $1/\mathrm{cm}^2 \cdot \mathrm{sr} \cdot \mathrm{s} \cdot \mathrm{keV}$) [7] $P_{\rm dyn}$ (MP – magnetopause, MSH – magnetosheath) obtained by the GE s/c. The Inset in the right bottom corner illustrates the observed interactions and magnetospheric boundaries

dard deviations σ. Correlation of the SPS appearance on DS with the average $|B_x|$ dominance ($|B_x|/|\mathbf{B}| > 0.5$, shadowed in Fig. 1) is seen from comparison of 1st and 2nd top panels. The spontaneous SPS appearance in the foreshock in front of the parallel BS is reproduced by the hybrid simulations [8]; the authors relay the Spontaneous Hot Flow Anomalies (SHFA, banded by the SPS [1]) with sunward streaming ions, generated at BS. These features agree both with the behavior of Transient Flux Events outlined in the early paper from the INTERBALL-1 s/c data [9], and with the recent statistical study of SHFA on THEMIS s/c [10].

Only less than 10% SPS on DS in Fig. 1 are sub-magnetosonic; in MSH the average magnetosonic Mach number, $\langle M_{ms}\rangle$, is $\sim 0.83 \pm 0.83$, for SPS $\langle M_{ms}\rangle_{\rm SPS} \sim 2.1 \pm 1$ with the maximum reaching 5.6. The average DS $\langle P_{\rm dyn}\rangle \sim 0.58$ (1.23-0) nP, for SPS $\langle P_{\rm dyn}\rangle_{\rm SPS} \sim 3.1 \pm 1$ with maximum 8.5 nP (for SW $\langle P_{\rm dyn}\rangle_{\rm SW} \sim 1.8 \pm 1$ nP). More than 30% SPS on DS do not correlate with the SW disturbances. C4–DS cross-correlation in $P_{\rm dyn}$ is less than 22%.

Spectral analysis. In Fig. 2 we present the Morlet wavelet power spectra of $P_{\rm dyn}$ for 03–09 UT (Inset) to compare foreshock and BS/MSH and for 09–14 UT to compare the signals in the most disturbed region. For frequencies < 0.15 mHz one can see the direct driving of MSH in the BS vicinity by SW, i.e. the similar spectral peaks are seen with attenuation in 3–5 times in MSH. At 0.22–0.25 mHz (see vertical dashed lines) SW disturbances are absent for most time. In the foreshock such

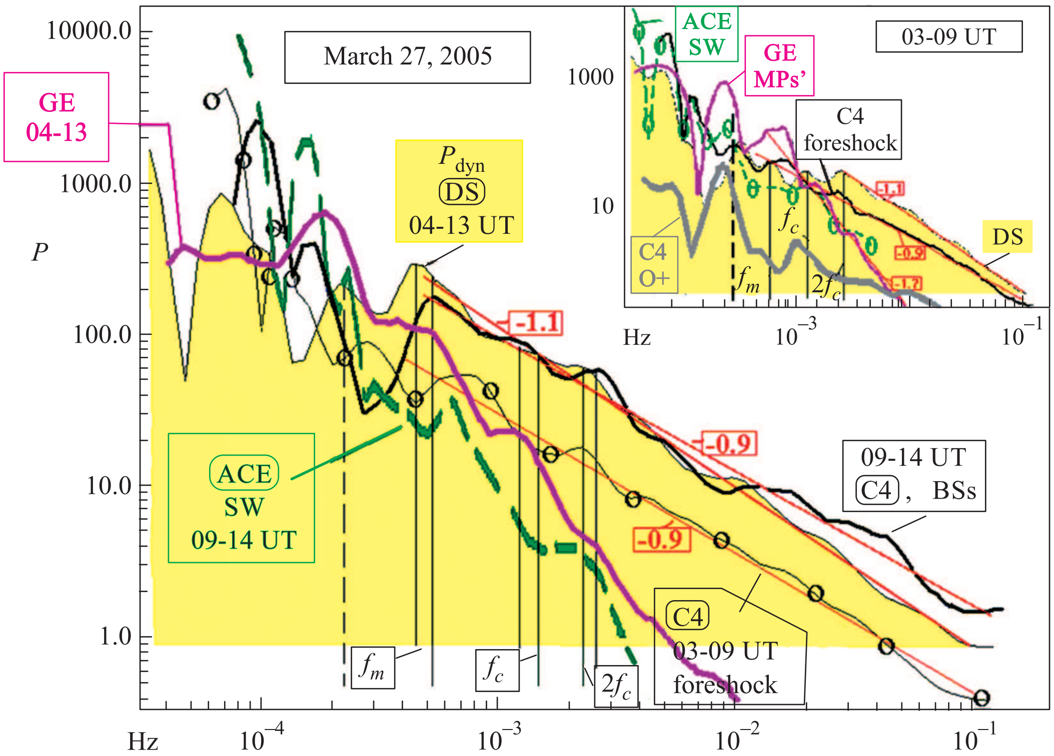

Fig. 2. Power spectra of $P_{\rm dyn}$ for the major regions in Fig. 1 on 4 s/c (see details in text). Inclined lines with squared values give average slopes. Inset: the same for 03–09 UT; grey lower curve – O^+ from C4 s/c

maximum appears first and, we suggest, it triggers the peak in MSH at ~ 0.23 mHz. A spectral maximum at ~ 0.2 mHz on GE has the similar nature, the frequency downshift can be due to the Doppler shift, which falls downtail with the characteristic scales rising. This resonance could correspond to an eigen frequency for generation of shocklets or for the shock front overturning [11]. GE MP crossings (see vertical dashed line) are strongly modulated by this frequency.

A striking feature is the quite similar spectral peak at ~ 0.2 mHz in the intensity of energetic O^+ (measured by RAPID on C4 [7], see bottom thick grey curve in Inset of Fig. 2), indicating the O^+ outflow from magnetosphere into SW. The cross-correlation $\sim 57\%$ is between the O^+ outflow on C4 and $P_{\rm dyn}$ on GE at 04–08 UT (the time delay is -2100 s). The average coherence at 04–08 UT between the O^+ outflow on C4 and $P_{\rm dyn}$ on GE is $\sim 85\%$ at 0.2–2 mHz, being $\sim 30\%$ at 03–20 UT. The magnetic pressure, P_b, is ~ 0.5 nP at the GE position (03–12 UT in Fig. 1), i.e. $P_b \ll P_{\rm dyn}$ in the MSH and the SW plasma transport can be controlled by the direct SPS penetration with an effectiveness up to an order of magnitude larger compared to other indirect mechanisms (cf. [1, 12]). A peak at frequency $f_m \sim (0.5-0.6)$ mHz is visible mostly near BS with a power growth up to 10 times above the SW level. Both DS and C4 register pumping of the energy into a BS resonance which we attribute to BS membrane mode (an eigen surface BS mode, cf. [13]). A foreshock maximum at ~ 0.8 mHz could trigger this resonance. Another, cavity, mode [14–16] (at the frequency f_c), has the following origin: MSH between BS and magnetosphere acts as a resonator for fast magnetosonic waves with eigen frequencies f_{cn} being roots of the Bessel function J_n [14–16]. Further to the higher frequencies, a cascade-like slope of about -1 is established. The MSH/SW spectra at 0.2–10 mHz provide the evidence that the inherent foreshock/BS/MSH processes are strongly dominant [16].

Magnetic power B_x and $|\mathbf{B}|$ spectra on C4 at 03–09, 09–14, 14–19 UT substantially differ from that of $P_{\rm dyn}$: magnetic peak at 0.25 mHz is close to the $P_{\rm dyn}$ minimum, the magnetic slope of -0.4 at 1–20 mHz falls down to -1.7 at 20–100 mHz. Thus, most previous studies of magnetic turbulence are not representative versus the presented here data.

Bi-spectral analysis. We proceed analysis of $P_{\rm dyn}$ from DS by calculating of the wavelet bi-spectra. This analysis is helpful to detect 3-wave interactions and to reveal indications how large-scale modes regulate the

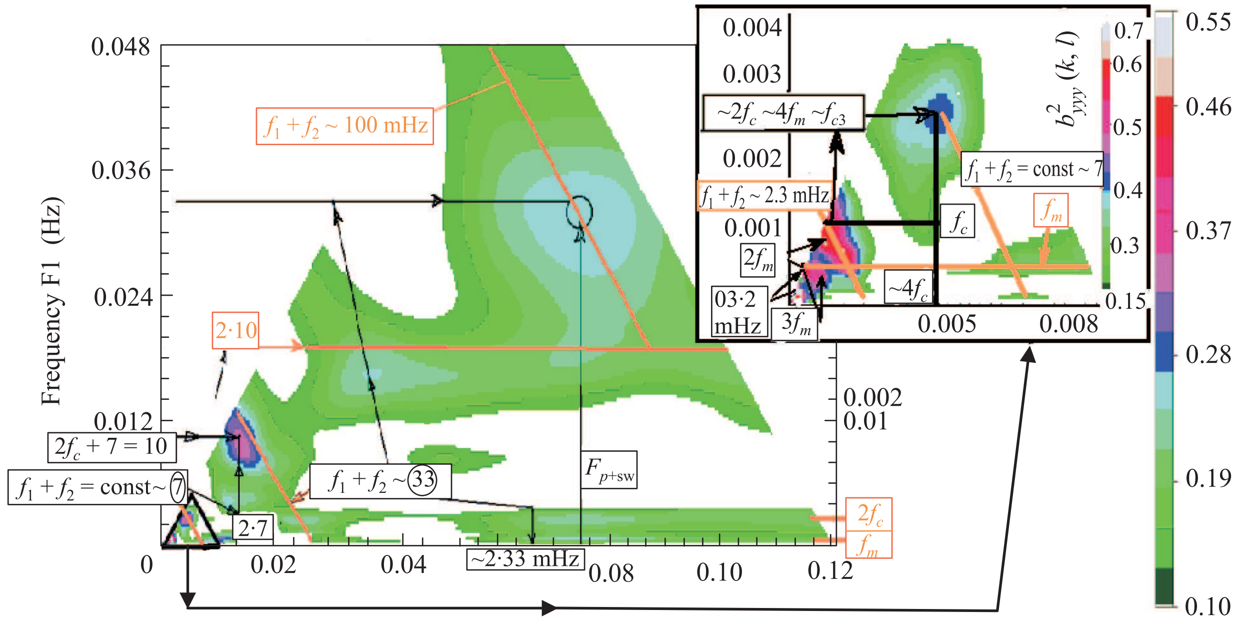

Fig. 3. Wavelet bicoherence (bi-spectra) of P_{dyn} from DS s/c at 04–13 UT on March 27, 2005 for 120 mHz range. Inset: the lower frequency blow-up showing mainly discrete cascades (see details in the text)

plasma turbulence and resultant transports (e.g. it is used to prove the coupling between turbulence and zonal flows in fusion devices [17]).

The bi-spectra proves the 2nd harmonic generation at $\sim 0.2 \pm 0.05$ mHz, which gives a large maximum (> 0.7, see the arrow root with the framed signature $3 \cdot 02$ mHz in the Inset). The 3d harmonic (at $\sim 0.6 \pm 0.07$ mHz, resonates with the BS membrane mode, $f_m \sim 0.6$ mHz, cf. [14]). At f_m one can see a discrete horizontal cascade in Fig. 3 with maximum at 29–33 mHz. We use the term "discrete cascade" for 3-wave interactions with the frequency law: $f_1 + f_2 = f_3$ when the signal at the same frequency (in our case at the plot Y axis $f_1 \sim$ marked in Fig. 3 by horizontal thick lines and by framed captures) interacts in turn with f_3 and so on. A maximum at $f_1 \sim f_m$ is at the plot axis $X \sim (1.4–1.8)$ mHz corresponding to the 4th harmonic generation of the f_m, which is close to the eigen frequency of the MSH cavity mode f_c. A maximum at $\sim f_c$ near the left upper edge indicates generation of the 2nd harmonic $f_c + f_c = 2f_c \sim 4f_m \sim f_{c3}$, i.e. "$2f_c$" could resonate with the 3d eigen cavity frequency f_{c3} (3d root of $\mathbf{J}_n$ [14–16]). The 4th harmonic of $f_m \sim 2.6$ mHz gives a bi-maximum $(2.6; 4.3)$ mHz, where 4.3 mHz is close to an eigen frequency f_{c4}. Both 2.6 and 4.3 mHz can in turn resonate with the cavity-modes for the BS and MP deformation substructures (the HFA or MP indentations produced by SPS being examples of such disturbances [1]), as well as with the cavity mode of the outer cusp throat [14]. At the plot axes $Y = f_c \sim 2.2–2.4$ and $X \sim 20$ mHz a horizontally-spread bi-maximum starts having maxima at $\sim(2.4; 30)$ and $(2.4; 75)$ mHz. The first one corresponds to a cascade $f_1 + f_2 \sim 33$ mHz, the prominent maximum at $\sim(10; 13)$ mHz is linked with the previous resonance $f_1 + f_2 \sim 7$ via $2f_c + 7 \sim 10$ and $2 \cdot 7 \sim 14 \pm 2$ mHz; a 2nd harmonic $\sim 2 \cdot 10$, in turn, gives origin to a horizontal cascade (the upper thick horizontal line). 33 mHz gives the maximum at $\sim(33; 75)$ mHz, 75 mHz being close to proton cyclotron frequency in SW ($F_{p+\mathrm{SW}}$). It produces the inclined cascade $f_1 + f_2 \sim 100$ mHz, which merges the horizontal one at $\sim 2 \cdot 10$ mHz. 2nd harmonic of 33 mHz (close to $F_{p+\mathrm{SW}}$) interacts with f_m, $2f_c$ and f_c horizontal cascades, representing the last step in transformation of the discrete into turbulent-like featureless cascades. While our cascade identification has a preliminary character, Fig. 3 demonstrates the presence of a number of discrete cascades. Finally in Fig. 3 the cascades become more featureless due to the resonances overlapping.

The described above features invoke the following picture: the SW disturbances at 0.15–10 mHz initiate discrete-like resonances, which get energy, most probably, directly from the SW. The interactions of the resonances step-by-step transform the quasi-discrete spectrum into the featureless one with a power-low spectrum having a slope of about -1 (cf. [1, 18]).

Statistical study. For the turbulent zone on DS (2nd top curve in Fig. 1), for the first time we study statistics based on $P_{\rm dyn}$. We analyzed a structure function scaling (exponent) [18] $\zeta(q)$ for the structure function $S_q(\tau) = \langle|\delta_\tau X(t)|^q\rangle \sim \tau^{\zeta(q)}$ (τ is the time increment) dependent on the function order q, where $\delta_\tau X(t) = X(t+\tau) - X(t)$, $X = P_{\rm dyn}/P_{\rm SW}$ on DS (see 2nd top panel in Fig. 1). The characterization of $\zeta(q)$ can be accomplished using the log-Poisson model of developed turbulence with intermittency (see [18]):

$$\zeta(q) = (1-\Delta)\frac{q}{3} + \frac{\Delta}{1-\beta}\left[1-(\beta)^{q/3}\right]. \qquad (1)$$

Fitting experimental data to the model (1) gives $\Delta = 0.3230$ and $\beta = 0.1844$. The time scaling of the mean-square displacement of particles $\langle\delta x^2\rangle \propto \tau^\gamma$, which we estimate using the formula [18]:

$$\gamma = 1 + \Delta(1-\beta)/\beta. \qquad (2)$$

Formula (2) gives $\gamma = 2.3$, i.e. $\langle\delta x^2\rangle \propto \tau^{2,3}$. It indicates the super-diffuse transport in super-ballistic regime with plasma acceleration between interactions with waves or SPS. The SPS provide interlink throughout MSH towards MP.

We further calculated the fitting parameters g_f and g for the cascade assuming one (4) and two (3) dimensional dissipative structures according to [18]:

$$\zeta_f(q) = \frac{q}{g_f^2} + 2\left[1-\left(\frac{1+g_f}{2g_f}\right)^{q/g_f}\right], \qquad (3)$$

$$\zeta(q) = q/g^2 + 1 - (1/g)^{q/g}. \qquad (4)$$

We obtained $g = 2.61$ and $g_f = 3.03$, this infers the dominating dissipative structures to be 2-dimensional (in contrast to previous studies [1, 18]), as suggested in [18].

We also study the SPS as extreme events. First, we define the threshold for an extreme event for the normalized DS pressure $P_{\rm dyn}/P_{\rm SW}$ as 3 standard deviations σ. The time-delays (waiting-time) Δt series have been constructed from intervals between successive extreme events in the signal. Typical power law exponent of the probability distribution function $P(\Delta t) \sim (\Delta t)^\varepsilon$ has $\varepsilon \approx -2.16$ (for a normal process with Gaussian statistics it should be ~ -1). Taking another criteria for the event selection: $P_{\rm dyn}/P_{\rm SW} > 1.2$ and > 1.5 gives the scaling parameters $\varepsilon \approx -2.03$ and -1.75 (in the 2nd top panel of Fig. 1 these criteria are marked by two horizontal lines). Thus, one gets the time-delay scaling approximately twice as high as one for Gaussian statistics [1, 18].

We checked that randomization of the phase of DS $P_{\rm dyn}$ signal from Fig. 1 results in disappearance of more than 84% of SPS and gives the scaling of $\varepsilon \approx -1.15$ (i.e. nearly Gaussian). It confirms that the SPS are the carriers for the anomalous non-Gaussian statistics.

In summary, determining $P_{\rm dyn}$ from data obtained by the four s/c we found:

1) in the case of horizontal SW magnetic field, more than 30% SPS observed at DS do not correlate with SW disturbances. Less than 50% of wave bursts at 0.2–75 mHz are triggered by disturbances in the SW (cf. [10]);

2) SW and foreshock disturbances trigger resonant oscillations in the outer magnetospheric regions (e.g. in the BS surface (membrane) and in the MSH (cavity modes)). These modes amplify the power of the upstream triggers up to an order of magnitude, taking the energy, most probably, directly from the SW kinetic energy. It is a feature newly found and reported here;

3) towards higher frequencies those resonances initiate, first, discrete 3-wave multiple cascades, become transformed into a featureless turbulent cascade (this is also shown for the first time);

4) the power spectrum slope at the high frequencies is of the order of unity which corresponds to "flicker" noise [16, 18]. The highest discrete frequency in the bi-spectra is the SW proton cyclotron frequency. This causes a deformation of the BS by disturbances reflected from the BS and returned by SW back towards the magnetosphere (see Inset in Fig. 1) including the BS reformation [11];

5) we found that the resonances at the magnetic barrier boundary modulate the direct penetration of SW plasma through the flank magnetopause due to SPS impacts (cf. [1]), and they also modulate the O^+ outflow from magnetosphere into SW (firstly shown here);

6) the SPS penetrate the BS at its deformed/inclined sites (see Inset in Fig. 1) where the BS normal direction declines away from the SW flow direction. Due to the weaker dissipation processes taking place in the BS with the declined normal, the BS Mach number decreases and super-magnetosonic flows (i.e. SPS) appear in the MSH [16, 19, 20], modulating all processes throughout the MSH;

7) the statistical properties of the SPS displays the intermittency features. Multifractal structures are formed in the boundary layers that result in a super-ballistic regime – in contrast to previous studies [18]. This finding corresponds to the multipoint spectrum analysis indicating that the SW kinetic energy is pumped into the resonances at the magnetospheric boundary.

A preliminary survey of DS and CLUSTER data reveals in more than half the observed cases with SPS the boundary resonances are detected. We found the indications that large scale eigen modes (at e.g. f_m and f_c) are coupled with the high frequency turbulence. This coupling is able to impact the plasma turbulence and resultant transports. Similar 3-wave coupling of eigen modes with the high frequency broadband turbulence have been outlined in the edge plasma of fusion devices [17].

We conclude that the modulated by resonance-like SPS interpenetration of the solar and Earth-produced plasma in and out through the magnetopause will have to be taken into account in attempt to predict the space weather. In view of similar statistical properties [1, 12, 18] the SPS-driven cascades looks to be also instructive for the development of turbulent cascades in different media including the laboratory plasma, e.g. intermittent plasma turbulence in fusion devices.

The work is supported by Ukrainian grant DFFD F53.2/039 and in frame of the Ukrainian NAS Program on space researches for 2012–2016, by grant MES RF 8413(8527), Czech Grant Agency P209/13/22367J. We appreciate the fruitful discussions with V. Krasnosielskikh, who provided an opportunity to use SWAN software from LPCE for the wavelet analysis.

1. S. Savin, E. Amata, L. Zelenyi, V. Lutsenko, J. Safrankova, Z. Nemecek, N. Borodkova, J. Buechner, P. W. Daly, E. A. Kronberg, J. Blecki, V. Budaev, L. Kozak, A. Skalsky, and L. Lezhen, Ann. Geophys. **30**, 1 (2012).
2. S. Savin, L. Zelenyi, E. Amata, J. Buechner, J. Blecki, A. Greco, S. Klimoa, R.E. Lopez, B. Nikutowski, E. Panov, J. Pickett, J.L. Rauch, S. Romanov, P. Song, A. Skalsky, V. Smirnov, A. Taktakishvili, P. Veltry, and G. Zimbardo, Planet. Space Sci. **53**, 133 (2005).
3. G. Gustafsson, M. André, T. Carozzi, A.I. Eriksson, C.-G. Fälthammar, R. Grard, G. Holmgren, J.A. Holtet, N. Ivchenko, T. Karlsson, Y. Khotyaintsev, S. Klimov, H. Laakso, P.-A. Lindqvist, B. Lybekk, G. Marklund, F. Mozer, K. Mursula, A. Pedersen, B. Popielawska, S. Savin, K. Stasiewicz, P. Tanskanen, A. Vaivads, and J-E.Wahlund, Ann. Geophys. **19**, 1219 (2001).
4. S. Savin, A. Skalsky, L. Zelenyi, V. Budaev, G. Consolini, R. Treumann, E. Lucek, J. Safrankova, Z. Nemecek, Y. Khotyaintsev, M. Andre, J. Buechner, H. Alleyne, P. Song, J. Blecki, J. L. Rauch, S. Romanov, S. Klimov, and A. Skalsky, Surv. Geophys. **26**, 95 (2005).
5. S. Savin, L. Zelenyi, S. Romanov, I. Sandahl, J. Pickett, E. Amata, L. Avanov, J. Blecki, E. Budnik, J. Büchner, C. Cattell, G. Consolini, J. Fedder, S. Fuselier, H. Kawano, S. Klimov, V. Korepanov, D. Lagoutte, F. Marcucci, M. Mogilevsky, Z. Nemecek, B. Nikutowski, M. Nozdrachev, M. Parrot, J. L. Rauch, V. Romanov, T. Romantsova, C. T. Russell, J. Safrankova, J. A. Sauvaud, A. Skalsky, V. Smirnov, K. Stasiewicz, J. G. Trotignon, and YU. Yermolaev, Ann. Geophys. **22**, 183 (2004).
6. L. V. Kozak, S. P. Savin, V. P. Budaev, V. A. Pilipenkob, and L. A. Lezhen, Geomagnetism and Aeronomy **52**(4), 445 (2012).
7. B. Wilken, P.W. Daly, U. Mall, G. Gustafsson1, M. André, T. Carozzi, A.I. Eriksson, C.-G. Fälthammar, R. Grard, G. Holmgren, J.A. Holtet, N. Ivchenko, T. Karlsson, Y. Khotyaintsev, S. Klimov, H. Laakso, P.-A. Lindqvist, B. Lybekk, G. Marklund, F. Mozer, K. Mursula, A. Pedersen, B. Popielawska, S. Savin, K. Stasiewicz, P. Tanskanen, A. Vaivads, and J-E.Wahlund, Ann. Geophys. **19**, 1355 (2001).
8. N. Omidi, H. Zhang, D. Sibeck, and D. Turner, J. Gephys. Res. **118**, 173 (2013).
9. Z. Nemecek, J. Safrankova, L. Prech, D. G. Sibeck, S. Kokubun, and T. Mukai, Geophys. Res. Lett. **25**, 1273 (1998).
10. M. O. Archer and T. S. Horbury, Ann. Geophys. **31**, 319 (2013).
11. V. Krasnoselskikh, M. Balikhin, S.N. Walker, V.S. Schwartz, D. Sundkvist, V. Lobzin, M. Gedalin, S. D. Bale, F. Mozer, J. Souce, Y. Hobara, and H. Comisel, in press, (2013).
12. S. Savin, E. Amata, L. Zelenyi, V. Budaev, G. Consolini, R. Treumann, E. Lucek, J. Safrankova, Z. Nemecek, Y. Khotyaintsev, M. Andre, J. Buechner, H. Alleyne, P. Song, J. Blecki, J. L. Rauch, S. Romanov, S. Klimov, and A. Skalsky, JETP Lett. **87**, 593 (2008).
13. F. Plaschke, K.-H. Glassmeier, H. U. Auster, H. U. O. D. Constantinescu, W. Magnes, V. Angelopoulos, D. G. Sibeck, and J. P. McFadden, J. Geophys. Res. **114**, A00C10 (2009).
14. V. V. Mishin, Planetary Space Science **29**, 359 (1981).
15. I. R. Mann, A. N. Wright, K. J. Mills, and V. M. Nakariakov, J. Geophys. Res. **104**, 333 (1999).
16. *Plasmennaya geliogeofizika (Plasma Heliogeophysics)*, ed. by L. M. Zelenyi and I. S. Veselovsky, Fizmatlit, M. (2008).
17. A. Fujisawa, T. Ido, A. Shimizu, S. Okamura, K. Matsuoka et al., Experimental Progress on Zonal Flow Physics in Toroidal Plasmas, NIFS-835 (2006).
18. V. P. Budaev, S. P. Savin, and L. M. Zelenyi, Physics – Uspekhi **54**(9), 875 (2011).
19. H. Hietala, T. V. Laitinen, K. Andreéová, R. Vainio, A. Vaivads, M. Palmroth, T. I. Pulkkinen, H. E. J. Koskinen, E. A. Lucek, and H. Re'me, Phys. Rev. Lett. **103**, 245001 (2009).
20. H. Hietala, N. Partamies, T. V. Laitinen, B. N. Clausen, G. Facskó, A. Vaivads, H. E. J. Koskinen, I. Dandouras, H. Rème, and E. A. Lucek, Ann. Geophys. **30**, 33 (2012).